Search for *CP* Violation in the Decay $B^0 \rightarrow D^{*\pm}D^{\mp}$

T. Aushev,[11] Y. Iwasaki,[7] K. Abe,[7] K. Abe,[39] I. Adachi,[7] H. Aihara,[41] M. Akatsu,[20] Y. Asano,[45] T. Aziz,[37] S. Bahinipati,[4] A. M. Bakich,[36] A. Bay,[16] I. Bedny,[1] U. Bitenc,[12] I. Bizjak,[12] S. Blyth,[24] A. Bondar,[1] A. Bozek,[25] M. Bračko,[18,12] J. Brodzicka,[25] P. Chang,[24] Y. Chao,[24] A. Chen,[22] W. T. Chen,[22] B. G. Cheon,[3] R. Chistov,[11] Y. Choi,[35] A. Chuvikov,[32] M. Danilov,[11] M. Dash,[46] L. Y. Dong,[9] J. Dragic,[19] A. Drutskoy,[4] S. Eidelman,[1] V. Eiges,[11] Y. Enari,[20] F. Fang,[6] S. Fratina,[12] N. Gabyshev,[1] A. Garmash,[32] T. Gershon,[7] G. Gokhroo,[37] B. Golob,[17,12] N. C. Hastings,[7] K. Hayasaka,[20] M. Hazumi,[7] T. Higuchi,[7] L. Hinz,[16] T. Hokuue,[20] Y. Hoshi,[39] S. Hou,[22] W.-S. Hou,[24] T. Iijima,[20] A. Imoto,[21] K. Inami,[20] A. Ishikawa,[7] H. Ishino,[42] R. Itoh,[7] M. Iwasaki,[41] J. H. Kang,[47] J. S. Kang,[14] S. U. Kataoka,[21] N. Katayama,[7] H. Kawai,[2] T. Kawasaki,[27] H. R. Khan,[42] H. J. Kim,[15] S. K. Kim,[34] K. Kinoshita,[4] P. Koppenburg,[7] S. Korpar,[18,12] P. Križan,[17,12] P. Krokovny,[1] C. C. Kuo,[22] A. Kuzmin,[1] Y.-J. Kwon,[47] J. S. Lange,[5] G. Leder,[10] S. H. Lee,[34] T. Lesiak,[25] J. Li,[33] S.-W. Lin,[24] D. Liventsev,[11] J. MacNaughton,[10] F. Mandl,[10] T. Matsumoto,[43] W. Mitaroff,[10] K. Miyabayashi,[21] H. Miyake,[29] H. Miyata,[27] R. Mizuk,[11] D. Mohapatra,[46] T. Mori,[42] T. Nagamine,[40] Y. Nagasaka,[8] E. Nakano,[28] M. Nakao,[7] H. Nakazawa,[7] Z. Natkaniec,[25] S. Nishida,[7] O. Nitoh,[44] S. Ogawa,[38] T. Ohshima,[20] T. Okabe,[20] S. Okuno,[13] S. L. Olsen,[6] W. Ostrowicz,[25] H. Ozaki,[7] P. Pakhlov,[11] H. Palka,[25] H. Park,[15] L. S. Peak,[36] L. E. Piilonen,[46] H. Sagawa,[7] Y. Sakai,[7] N. Sato,[20] T. Schietinger,[16] O. Schneider,[16] J. Schümann,[24] A. J. Schwartz,[4] S. Semenov,[11] K. Senyo,[20] M. E. Sevior,[19] H. Shibuya,[38] A. Somov,[4] N. Soni,[30] R. Stamen,[7] M. Starič,[12] K. Sumisawa,[29] T. Sumiyoshi,[43] O. Tajima,[7] F. Takasaki,[7] N. Tamura,[27] M. Tanaka,[7] G. N. Taylor,[19] Y. Teramoto,[28] K. Trabelsi,[6] T. Tsukamoto,[7] S. Uehara,[7] T. Uglov,[11] K. Ueno,[24] S. Uno,[7] G. Varner,[6] K. E. Varvell,[36] S. Villa,[16] C. C. Wang,[24] C. H. Wang,[23] B. D. Yabsley,[46] A. Yamaguchi,[40] Y. Yamashita,[26] J. Ying,[31] Y. Yuan,[9] S. L. Zang,[9] J. Zhang,[7] L. M. Zhang,[33] Z. P. Zhang,[33] V. Zhilich,[1] and D. Žontar[17,12]

(Belle Collaboration)

[1]*Budker Institute of Nuclear Physics, Novosibirsk*
[2]*Chiba University, Chiba*
[3]*Chonnam National University, Kwangju*
[4]*University of Cincinnati, Cincinnati, Ohio 45221*
[5]*University of Frankfurt, Frankfurt*
[6]*University of Hawaii, Honolulu, Hawaii 96822*
[7]*High Energy Accelerator Research Organization (KEK), Tsukuba*
[8]*Hiroshima Institute of Technology, Hiroshima*
[9]*Institute of High Energy Physics, Chinese Academy of Sciences, Beijing*
[10]*Institute of High Energy Physics, Vienna*
[11]*Institute for Theoretical and Experimental Physics, Moscow*
[12]*J. Stefan Institute, Ljubljana*
[13]*Kanagawa University, Yokohama*
[14]*Korea University, Seoul*
[15]*Kyungpook National University, Taegu*
[16]*Swiss Federal Institute of Technology of Lausanne, EPFL, Lausanne*
[17]*University of Ljubljana, Ljubljana*
[18]*University of Maribor, Maribor*
[19]*University of Melbourne, Victoria*
[20]*Nagoya University, Nagoya*
[21]*Nara Women's University, Nara*
[22]*National Central University, Chung-li*
[23]*National United University, Miao Li*
[24]*Department of Physics, National Taiwan University, Taipei*
[25]*H. Niewodniczanski Institute of Nuclear Physics, Krakow*
[26]*Nihon Dental College, Niigata*
[27]*Niigata University, Niigata*
[28]*Osaka City University, Osaka*
[29]*Osaka University, Osaka*
[30]*Panjab University, Chandigarh*
[31]*Peking University, Beijing*
[32]*Princeton University, Princeton, New Jersey 08545*
[33]*University of Science and Technology of China, Hefei*

[34]Seoul National University, Seoul
[35]Sungkyunkwan University, Suwon
[36]University of Sydney, Sydney NSW
[37]Tata Institute of Fundamental Research, Bombay
[38]Toho University, Funabashi
[39]Tohoku Gakuin University, Tagajo
[40]Tohoku University, Sendai
[41]Department of Physics, University of Tokyo, Tokyo
[42]Tokyo Institute of Technology, Tokyo
[43]Tokyo Metropolitan University, Tokyo
[44]Tokyo University of Agriculture and Technology, Tokyo
[45]University of Tsukuba, Tsukuba
[46]Virginia Polytechnic Institute and State University, Blacksburg, Virginia 24061
[47]Yonsei University, Seoul

We report a search for CP-violating asymmetry in $B^0 \to D^{*\pm} D^{\mp}$ decays. The analysis employs two methods of B^0 reconstruction: full and partial. In the full reconstruction method all daughter particles of the B^0 are required to be detected; the partial reconstruction technique requires a fully reconstructed D^- and only a slow pion from the $D^{*+} \to D^0 \pi^+_{\mathrm{slow}}$ decay. From a fit to the distribution of the time interval corresponding to the distance between two B meson decay points we calculate the CP-violating parameters and find the significance of nonzero CP asymmetry to be 2.7 standard deviations.

In the standard model (SM), CP violation arises from the Kobayashi-Maskawa (KM) phase [1] in the weak interaction quark-mixing matrix. Comparisons between SM expectations and measurements in various modes are important to test the KM model. The $B^0 \to D^{*\pm} D^{\mp}$ modes are of particular interest since large CP violation effects are expected in these decays [2]. Although the $D^{*\pm} D^{\mp}$ final states are not CP eigenstates, they can be produced in the decays of both B^0 and $\bar{B}^0$ with comparable amplitudes: the interference between amplitudes of the direct transition and that via $B\bar{B}$ mixing results in CP violation. These decays are dominated by the tree $b \to c\bar{c}d$ transition; thus CP violation measurements are sensitive to the angle ϕ_1. However, the $b \to d$ penguin diagram also contributes to this final state and contains a different weak phase. Therefore this contribution results in both direct CP violation and a deviation of the mixing-induced CP violation parameter from $\sin 2\phi_1$. The Cabibbo suppressed decays $B^0 \to D^{*\pm} D^{\mp}$ were first observed by Belle [3], and have been confirmed by $BABAR$ [4].

The probability for a B meson to decay to $D^{*\pm} D^{\mp}$ at time Δt can be expressed in terms of five parameters, $\mathcal{A}$, $S_{\pm}$, and $C_{\pm}$:

$$\mathcal{P}^{\pm}_{D^* D}(\Delta t) = (1 \pm \mathcal{A}) \frac{e^{-|\Delta t|/\tau_{B^0}}}{8\tau_{B^0}} \{1 + q[S_{\pm} \sin(\Delta m_d \Delta t) - C_{\pm} \cos(\Delta m_d \Delta t)]\}. \quad (1)$$

Here the $+$ $(-)$ sign represents the $D^{*+} D^-$ $(D^{*-} D^+)$ final state, and the b-flavor charge $q = +1$ (-1) when the tagging B meson is a B^0 $(\bar{B}^0)$. The time-integrated asymmetry $\mathcal{A}$ between the rates to $D^{*+} D^-$ and $D^{*-} D^+$

is defined as

$$\mathcal{A} = \frac{N_{D^{*+} D^-} - N_{D^{*-} D^+}}{N_{D^{*+} D^-} + N_{D^{*-} D^+}}. \quad (2)$$

In the case of negligible penguin contributions [2,5], the parameters $S_{\pm}$ can be related to the weak phase difference ($\sin 2\phi_1$ in the SM), the strong phase difference (δ), and the ratio of tree amplitudes to the $D^{*+} D^-$ and $D^{*-} D^+$ final states. If $\delta = 0$ and equal amplitudes are assumed, one expects that $\mathcal{A} = 0$, $C_+ = C_- = 0$, and $S_+ = S_- = -\sin 2\phi_1$.

The analysis described here is based on 140 fb^{-1} of data, corresponding to 152×10^6 $B\bar{B}$ pairs, collected with the Belle detector [6] at the KEKB asymmetric energy storage rings [7]. Two reconstruction techniques, full and partial, are used to increase the reconstruction efficiency. The event selection is similar to that in our previous publication [3]; however, some requirements are relaxed in order to increase the size of the sample used to extract the CP violation parameters. The full reconstruction method allows extraction of the signal decay with high purity, but, due to the small branching fractions of charmed meson decays into reconstructable final states, results in a low efficiency. In the partial reconstruction method, a D^- meson is fully reconstructed while only the slow pion (π^+_{slow}) is required to be detected from the decay $D^{*+} \to D^0 \pi^+_{\mathrm{slow}}$.

Neutral D mesons are reconstructed in five decay modes: $K^- \pi^+$, $K^- \pi^+ \pi^+ \pi^-$, $K^- \pi^+ \pi^0$, $K_S \pi^+ \pi^-$, and $K^+ K^-$ [8]. Charged D mesons are reconstructed via decays into $K^+ \pi^- \pi^-$, $K_S \pi^-$, and $K^+ K^- \pi^-$. The selected combinations are fitted to a common vertex and a vertex quality requirement is applied to reduce combina-

torial background. A ± 15 MeV/c^2 interval around the nominal D mass is used to select D meson candidates for all modes except $D^0 \rightarrow K^- \pi^+ \pi^0$, for which ± 24 MeV/c^2 is used ($\sim 3\sigma$ in each case). The selected charmed meson candidates are then subjected to mass-vertex constrained fits to improve their momentum and vertex resolution. We refer to a D candidate as having valid vertex reconstruction if it is formed by at least two tracks with hits in the silicon vertex detector. To suppress feed-down from the Cabibbo allowed decay $\bar{B}^0 \rightarrow D^{*+} D_s^{(*)-}$ due to K/π misidentification, we apply a D_s^- veto for the $D^- \rightarrow K^+ \pi^- \pi^-$ and $K_S \pi^-$ channels: if a pion candidate can also be identified as a kaon, and if, after reassignment of the kaon mass, the invariant mass of the combination is within ± 15 MeV/c^2 of the nominal D_s^- mass, the combination is rejected. This requirement suppresses the $\bar{B}^0 \rightarrow D^{*+} D_s^{(*)-}$ background by a factor of 10 with signal efficiency of 98%. The D^{*+} candidates are formed from $D^0 \pi_{\text{slow}}^+$ combinations with invariant masses within ± 2 MeV/c^2 of the nominal D^{*+} mass.

In the full reconstruction method we define B^0 candidates as combinations of oppositely charged D^{*+} and D^- candidates, where at least one of the D^- or the D^0 from the D^{*+} decay has valid vertex reconstruction. The signal is identified using the c.m. system energy difference $\Delta E = E_B^* - E_{\text{beam}}$ and the beam-energy constrained mass $M_{\text{bc}} = \sqrt{E_{\text{beam}}^2 - P_B^{*2}}$, where E_B^* (P_B^*) is the energy (momentum) of the B candidate in the c.m. and E_{beam} is the c.m. beam energy. B^0 candidates are preselected by requiring $|\Delta E| < 100$ MeV and $M_{\text{bc}} > 5.21$ GeV/c^2. In the case of multiple B^0 candidates in this region a single candidate per event is selected based on the minimum sum of $\chi^2/$DOF of the fits to intermediate charmed mesons. The scatter plot of ΔE vs M_{bc} and the ΔE and M_{bc} projections are shown in Fig. 1. In the M_{bc} projection B^0 candidates are selected from the $|\Delta E| < 20$ MeV re-

FIG. 1.   Kinematic distributions of $B^0 \rightarrow D^{*\pm} D^{\mp}$ candidates: (a) scatter plot of ΔE vs M_{bc}; (b),(c) ΔE and M_{bc} projections; (d) $\cos\theta$ determined from M_{bc} fits in the data (points with error bars) and in the signal MC (histogram). The curves represent the fit described in the text.

gion; the ΔE distribution is plotted for the region $M_{\text{bc}} > 5.27$ GeV/c^2. A fit to the M_{bc} distribution with a Gaussian representing the signal contribution and an ARGUS function [9] parameterizing the background finds a signal yield of 161 ± 16 events. A fit to the ΔE distribution is performed using a double Gaussian to parametrize the signal, while the background is described by a linear function. This fit yields 149 ± 18 signal events. The $\cos\theta$ distribution, where θ is a decay angle in the D^{*+} rest frame relative to the boost direction, for the candidates from the $|\Delta E| < 20$ MeV and $M_{\text{bc}} > 5.27$ GeV/c^2 regions determined from M_{bc} fits is shown in Fig. 1(d) and is in good agreement with the Monte Carlo (MC) expectation.

In the partial reconstruction analysis we define B candidates as combinations of D^- with valid vertex reconstruction and π_{slow}^+. As in our previous publication [3], the angle α between the D^- and π_{slow}^+ c.m. momenta, and the D^{*+} helicity angle θ, calculated using kinematic constraints, is used to identify the studied decay. We use the $D^- \rightarrow K^+ \pi^- \pi^-$ decay mode only. In addition, the D^- c.m. momentum is required to lie in the interval $1.63 < P_{D^-}^* < 1.97$ GeV/c, and the c.m. momentum of π_{slow}^+ is required to be smaller than 0.2 GeV/c. Both momentum intervals correspond to the kinematic limits for the studied decay. In order to make the fully and partially reconstructed samples statistically independent, π_{slow}^+ is rejected if, after being combined with any D^0 in the event, it forms a D^{*+} candidate. The presence of a lepton (ℓ_{tag}) in the event is required to provide flavor tagging, suppress the continuum background to a negligible level, and also reduce the combinatorial $B\bar{B}$ background. Charged tracks with c.m. momenta in the range $1.1 < P_{\ell_{\text{tag}}}^* < 2.3$ GeV/c, which are identified as muons or electrons, are considered as leptons. A large fraction of the selected $D^- \ell_{\text{tag}}$ combinations originate from the decay of the same B meson: $B \rightarrow D^- \ell^+ X$. This background is removed by a kinematic requirement that D^- and ℓ_{tag} do not originate from the same B:

$$\frac{(E_{\text{beam}} - E_{D\ell_{\text{tag}}}^*)^2 - P_B^{*2} - P_{D\ell_{\text{tag}}}^{*2}}{2 P_B^* P_{D\ell_{\text{tag}}}^*} < -1.1, \quad (3)$$

where $E_{D\ell_{\text{tag}}}^*$ ($P_{D\ell_{\text{tag}}}^*$) is the c.m. energy (momentum) of the $D^- \ell_{\text{tag}}$ combination. The efficiency of this requirement for the signal is estimated from MC simulation to be 87%, while the background is suppressed by a factor greater than 2. This requirement also removes leptons produced from the unreconstructed D^0 in the signal decay, an additional source of mistagging. We select partially reconstructed B^0 candidates by requiring $\cos\alpha < 0$ and $|\cos\theta| < 1.05$. In the case of multiple candidates, the $D^- \pi_{\text{slow}}^+$ combination with the best probability of the D^- vertex fit or the largest $|\cos\theta|$ is selected. The ex-
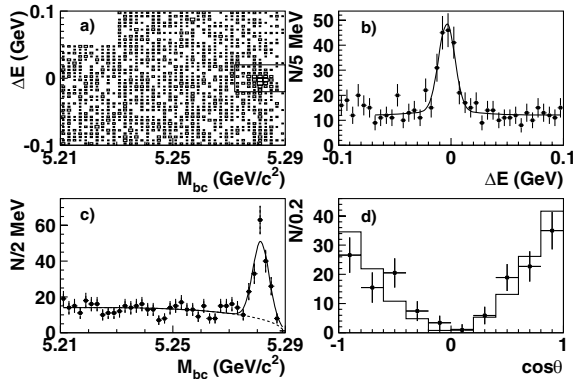
pected number of signal events in the partial reconstruction sample is calculated from the full reconstruction signal yield relying on the MC ratio of full and partial reconstruction efficiencies. We estimate $N_{\text{partial}} = 133 \pm 13$ and use this number to fix the signal fraction in later fits.

We cross-check this result by estimating the signal fraction from the data. The distributions of $\cos\alpha$ for two regions of $\cos\theta$ are shown in Fig. 2, after imposing a tight requirement of ± 8 MeV/c^2 ($\sim 2\sigma$) on the D^- mass. The first region $0.50 < |\cos\theta| < 1.05$ [Fig. 2(a)] is signal enriched due to the D^{*+} polarization; the second region $|\cos\theta| < 0.50$ [Fig. 2(b)] is dominated by background. In a simultaneous fit to the two $\cos\alpha$ distributions the signal shapes are fixed from the MC. The combinatorial background is parametrized by a second order polynomial function. The contributions from $\bar{B}^0 \to D^{*+} D_s^{(*)-}$ and $B^0 \to D^{*+} D^{*-}$ are fixed from the MC simulation. The fit yields 137 ± 39 signal events, in good agreement with the yield expected from the full reconstruction analysis.

In the full reconstruction method, charged tracks that are not associated with the reconstructed $B^0 \to D^{*\pm} D^{\mp}$ are used to identify the flavor of the signal B^0 [10]. Events are divided into six subsamples of the parameter r, which is an event-by-event, MC-determined flavor-tagging quality factor that ranges from $r = 0$ for no flavor discrimination to $r = 1$ for unambiguous flavor assignment. The wrong-tag fraction and difference between B^0 and $\bar{B}^0$ decays in each interval (w_i and Δw_i, $i = 1, 6$) are fixed using a data sample of self-tagged B^0 decay modes. In the partial reconstruction case, flavor tagging is provided by the high momentum lepton required in the event; the wrong-tag fraction is determined from data as discussed below.

The proper-time difference between the reconstructed and tagged B decay is calculated as $\Delta t = (z_{D^*D} - z_{\text{tag}})/\beta\gamma c$, where z_{D^*D} and z_{tag} are the z coordinates of the two B decay vertices and $\beta\gamma = 0.425$ is the Lorentz boost factor at KEKB. In the full reconstruction method we determine the B^0 signal vertex by fitting the momentum vectors of D^- and/or D^0 candidates with well-reconstructed vertices with the constraint of the interaction region profile. The tagging B vertex is found using well-reconstructed charged tracks not assigned to the
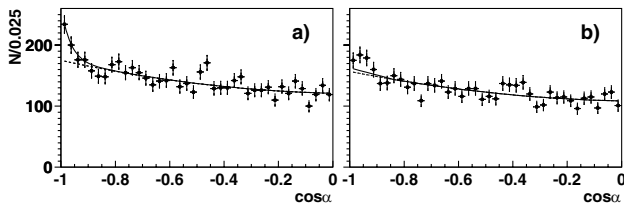
signal B^0 and excluding tracks that form a K_S candidate. The signal resolution function parameters are obtained from the Δt fit to the B^0 lifetime for the events from the signal region. The tagging B^0 vertex resolution function is fixed from [10]. In the partial reconstruction method, the signal and tagging B^0 vertices are reconstructed using the D^- candidate and ℓ_{tag}, respectively. In this case, both the resolution function parameters and the wrong-tag fraction are extracted from the data using a sample of $B^0 \to D^- \ell^+ \nu X$ decays tagged with a high momentum lepton. The $D^- \ell^+$ combinations are required to originate from the same B decay based on the recoil mass against the $D^- \ell^+$ system and its c.m. momentum. The selected $D^- \ell^+$ combinations are almost pure $B^0 \to D^- \ell^+ \nu$ signal events with a small admixture of $B^0 \to D^{*-}(D^- \pi^0)\ell^+ \nu$; the latter process is also considered as signal. A small contribution from combinatorial background under the D^- peak is estimated using D^- mass sidebands. The D^-, ℓ^+, and ℓ_{tag} vertices (z_{D^-}, z_{ℓ^+}, and $z_{\ell_{\text{tag}}}$) are reconstructed using identical procedures to those used in the partial reconstruction method. The resolution function is extracted from an unbinned maximum likelihood fit to the $\Delta t_\ell \equiv (z_{D^-} - z_\ell)/\beta\gamma c$ distribution. The wrong-tag fraction is found from a fit to $\Delta t_{\text{tag}} \equiv (z_{D^-} - z_{\text{tag}})/\beta\gamma c$ to be $w = (6.1 \pm 0.9)\%$. As a cross-check, the B^0 lifetime and mixing parameter Δm_d are also measured from the fit to the Δt_{tag} distribution to be 1.48 ± 0.04 ps and 0.52 ± 0.02 ps^{-1}, respectively, consistent with [11].

In the full reconstruction method, the signal region is defined as $|\Delta E| < 50$ MeV and $M_{\text{bc}} > 5.27$ GeV/c^2 and contains 360 events with 46% signal purity. In the partial reconstruction method, the signal region is chosen as $|M_{K^+\pi^-\pi^-} - M_{D^-}| < 15$ MeV/c^2, $\cos\alpha < -0.9$, and $|\cos\theta| < 1.05$. The total number of selected events is 2174 with 6% signal purity.

We determine the CP violation parameters from an unbinned maximum likelihood fit to the Δt distribution. The signal probability density function is given by Eq. (1) with effects due to mistagging taken into account. The resolution function R_{D^*D} is formed by convolving four components: the detector resolutions for z_{D^*D} and z_{tag}, the shift in the z_{tag} vertex position due to secondary tracks originating from charmed particle decays, and the smearing due to the kinematic approximation used to convert Δz to Δt [10]. For each event we define the following likelihood value:

FIG. 2. Distributions of $\cos\alpha$ for (a) $0.50 < |\cos\theta| < 1.05$ and (b) $|\cos\theta| < 0.50$. The fit functions are shown with solid lines; the combinatorial backgrounds are presented by dashed lines.

$$P_i = \int \left[\frac{f_{D^*D}}{f_{D^*D} + f_{\text{bg}}} \mathcal{P}_{D^*D}(\Delta t') R_{D^*D}(\Delta t_i - \Delta t') \right.$$
$$\left. + \frac{f_{\text{bg}}}{f_{D^*D} + f_{\text{bg}}} \mathcal{P}_{\text{bg}}(\Delta t') R_{\text{bg}}(\Delta t_i - \Delta t') \right] d\Delta t', \quad (4)$$

where signal (f_{D^*D}) and background (f_{bg}) fractions are calculated as functions of the following variables: ΔE and M_{bc} (full reconstruction); M_{D^-} and $\cos\alpha$ (partial

TABLE I. Fit results.

	Full rec.	Partial rec.	Combined
$\mathcal{A}$	$+0.03 \pm 0.09$	$+0.16 \pm 0.18$	$+0.07 \pm 0.08$
S_-	-1.17 ± 0.48	-0.65 ± 0.79	-0.96 ± 0.43
C_-	$+0.33 \pm 0.29$	$+0.11 \pm 0.45$	$+0.23 \pm 0.25$
S_+	-0.25 ± 0.52	-0.92 ± 0.58	-0.55 ± 0.39
C_+	-0.34 ± 0.27	-0.39 ± 0.38	-0.37 ± 0.22

reconstruction); $\cos\theta$ (both cases). The signal distributions of the variables used for f_{D^*D} parametrization are determined from the MC simulation. The background parameters are obtained from the data.

In the full reconstruction, the background Δt shape is fixed using the large $M_{\rm bc}$-ΔE region excluding the signal region. For the partial reconstruction the background contains a combinatorial component, for which the shape is obtained from D^- mass sidebands ($30 \text{ MeV}/c^2 < |M_{K^+\pi^-\pi^-} - M_{D^-}| < 60 \text{ MeV}/c^2$), and a component containing a real D^-, which may come from B decay. The shape of the latter includes a mixing term and is obtained from a sideband ($-0.8 < \cos\alpha < 0.0$).

Finally, the results for the CP violation parameters $\mathcal{A}$, $S_\pm$, and $C_\pm$ obtained from the individual fits to the statistically independent full reconstruction and partial reconstruction samples, as well as the result of the combined fit, are summarized in Table I. We calculate the combined statistical significance of CP violation to be 2.7σ. The significance is defined as $\sqrt{-2\ln(L_0/L_{\max})}$, where $L_{\max}$ is the likelihood returned by the combined fit and L_0 is determined from a fit with the parameters $\mathcal{A}$, $S_\pm$, and $C_\pm$ constrained to the values corresponding to no CP violation: $\mathcal{A} = 0$, $S_+ = -S_-$, and $C_+ = -C_-$.

The Δt distributions for the subsamples having the best signal and tagging quality ($f_{D^*D} > 0.1$ and $r > 0.5$) after background subtraction are shown in Figs. 3(a) and 3(b) for the full and partial reconstruction methods, respectively.

The systematic error is dominated by the uncertainties in the signal fraction (± 0.07 for $S_\pm$ and ± 0.03 for $C_\pm$), wrong-tag fraction (± 0.05 for $S_\pm$ and ± 0.03 for $C_\pm$), resolution function parametrization (± 0.05 for $S_\pm$ and ± 0.02 for $C_\pm$), and vertexing (± 0.05 for $S_\pm$ and ± 0.01 for $C_\pm$). Other contributions come from the correlated backgrounds and signal box definition. The result is consistent with [4]. We perform a number of cross-checks for our measurement. Using an ensemble of MC pseudoexperiments, we check both the linearity of the fitting procedure and the reliability of the statistical errors returned by the CP fit. A similar CP violation study is performed with self-tagged $\bar{B}^0 \to D^{*+}D_s^-$ decay using both full and partial reconstruction techniques. The combined fit yields $\mathcal{A} = 0.00 \pm 0.03$, $S_- = +0.08 \pm 0.12$, $C_- = -1.11 \pm 0.07$, $S_+ = +0.00 \pm 0.12$, and $C_+ =$
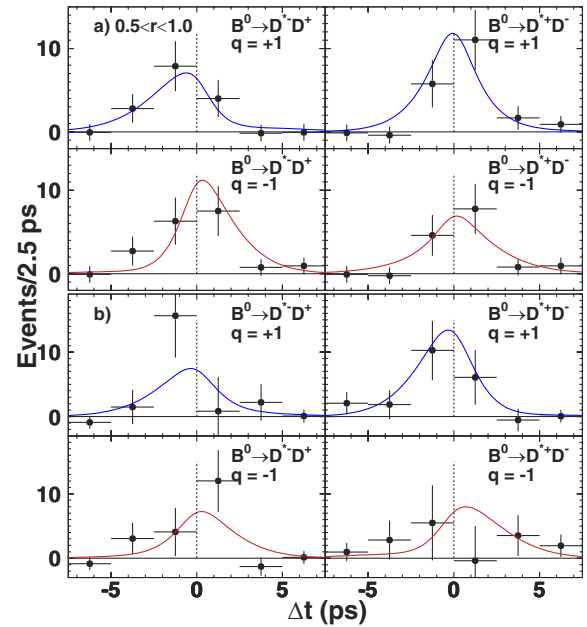

FIG. 3 (color online). Background subtracted Δt distributions in the (a) full and (b) partial reconstruction methods. The curves show the result of the fits.

$+1.12 \pm 0.07$, consistent with the expected values $\mathcal{A} = 0$, $S_\pm = 0$, and $C_+ = -C_- = 1$.

In summary, we have performed a search for the CP-violating asymmetry in the decay $B^0 \to D^{*\pm}D^\mp$ using two methods of B^0 reconstruction. From the combined fit to the data we have measured $\mathcal{A} = +0.07 \pm 0.08 \pm 0.04$, $S_- = -0.96 \pm 0.43 \pm 0.12$, $C_- = +0.23 \pm 0.25 \pm 0.06$, $S_+ = -0.55 \pm 0.39 \pm 0.12$, and $C_+ = -0.37 \pm 0.22 \pm 0.06$. These are the most precise measurements of these parameters to date. The significance of nonzero CP violation in $B^0 \to D^{*\pm}D^\mp$ is 2.7σ.

[1] M. Kobayashi and T. Maskawa, Prog. Theor. Phys. **49**, 652 (1973).
[2] R. Aleksan *et al.*, Phys. Lett. B **317**, 173 (1993).
[3] Belle Collaboration, K. Abe *et al.*, Phys. Rev. Lett. **89**, 122001 (2002).
[4] *BABAR* Collaboration, B. Aubert *et al.*, Phys. Rev. Lett. **90**, 221801 (2003).

[5] Z.-Z. Xing, Phys. Lett. B **443**, 365 (1998).

[6] Belle Collaboration, A. Abashian *et al.*, Nucl. Instrum. Methods Phys. Res., Sect. A **479**, 117 (2002).

[7] S. Kurokawa and E. Kikutani, Nucl. Instrum. Methods Phys. Res., Sect. A **499**, 1 (2003).

[8] The inclusion of charge conjugate modes is implied throughout this Letter.

[9] ARGUS Collaboration, H. Albrecht *et al.*, Phys. Lett. B **229**, 304 (1989).

[10] Belle Collaboration, K. Abe *et al.*, hep-ex/0308036; Belle Collaboration, H. Kakuno *et al.*, hep-ex/0403022; Belle Collaboration, K. Abe *et al.*, Phys. Rev. D **66**, 071102 (2002).

[11] S. Eidelman *et al.*, Phys. Lett. B **592**, 1 (2004).